

## VULNERABILITY ASSESSMENT OF RC BUILDINGS TO LANDSLIDE DISPLACEMENTS. APPLICATION TO CORNIGLIO CASE HISTORY, ITALY

Stavroula D. Fotopoulou<sup>1</sup>, Alberto Callerio<sup>2</sup>, Kyriazis D. Pitilakis<sup>1</sup>

<sup>1</sup> Aristotle University of Thessaloniki  
Department of Civil Engineering, Thessaloniki, Greece  
sfotopou@civil.auth.gr, kpitilak@civil.auth.gr

<sup>2</sup> Studio Geotecnico Italiano srl  
Via Ripamonti 89, 20141 Milan, Italy  
a.callerio@studiogeotecnico.it

**Keywords:** Landslide Vulnerability, RC Buildings, Corniglio Case History, Fragility Curves, Numerical Analysis.

**Abstract.** *The present study shows an application to a specific case history (the Corniglio village major landslide) of a recently proposed analytical method for the vulnerability assessment of RC buildings subjected to earthquake induced slow-moving slides [5]. In particular, the method is applied to a representative building which suffered considerable damage by the landslide movement [7]. The main goal is to verify the reliability and applicability of the proposed procedure and of the respective fragility curves through the comparison of the numerical prediction with the observed building damage. Two different approaches of increased complexity were followed for the fragility analysis of the building. At first, two sets of the already developed fragility curves derived from an extensive parametric analysis [6] are selected as the more representative of the Corniglio case history. Thus, the results obtained from their application are compared with the observed building damage, for the measured level of building displacement. The direct comparison carried out proved that the proposed fragility curves could in general capture the performance of the studied RC building when affected by a landslide induced displacement. Then, to enhance the effective implementation of the proposed methodological framework within a more general probabilistic risk assessment study, appropriate fragility curves were defined for a specific building in Corniglio village by means of a straightforward numerical computation. In particular, a two-step numerical approach which includes soil structure dynamic analysis and a structural pseudo-static calculation was followed to assess the expected building induced stress and damage [5]. As in the previous step, the obtained fragility curves were tested through their comparison with the observed building damage data, for a given level of landslide displacement.*

## 1 INTRODUCTION

Landslides constitute one of the most destructive natural hazards causing considerable damage and fatalities particularly in mountainous environments. Therefore, the estimation of the risk level associated with slope failures became a fundamental task in developing proper disaster management and mitigation policies.

One of the most important challenges in evaluating the landslide risk is represented by a comprehensive evaluation of vulnerability of the exposed elements. In the literature, several different approaches to assess the vulnerability of the affected assets only in a qualitative manner or by using rather simplistic empirical or expert-judgment approaches were proposed [1, 2, 3]. This is principally due to the scarcity of quantitative damage data and the inherent uncertainties associated with them [4]. The heterogeneity of potentially vulnerable elements to similar landslide mechanisms, the type of landslide (e.g. rockfalls, debris flows, earth slides etc.) and their characteristics (e.g. size, shape, velocity, momentum), not forgetting the numerous categories of damages and their inherent dynamic nature, contributed to the insufficient and somewhat subjective treatment of the vulnerability to landslide induced movements.

Within the framework of SAFELAND European project (<http://www.safeland-fp7.eu>), Fotopoulou and Pitilakis [5] developed an analytical method to quantify the vulnerability of reinforced concrete buildings subjected to earthquake induced, slow-moving slides. There, vulnerability is described through the appropriate definition of fragility curves which provide the conditional probability to exceed a certain damage state under a landslide event of a given type and intensity. Several sets of fragility curves for RC low-rise, frame structures were proposed by the same authors [6] on the basis of an extensive numerical parametric analysis carried out on different slope geometry, soil conditions and distance of the building with respect to the slope's crest.

In this paper, stemming from a high-quality set of experimental and observational data in terms of landslide induced ground and building displacement, together with measured building damage, made available and post-processed for a population of buildings in the village of Corniglio in the North-Western Italian Appennines [7], an application of the recently published analytical methodology is presented [5]. More specifically, the aim of the research was twofold: (a) to explore the reliability of the fragility curves derived via extensive parametric investigation [6] through their comparison with the observed damage data for a representative RC frame building under the measured level of ground and building displacement, and (b) to enhance the applicability band of the proposed methodological framework [5] by comparison of appropriate fragility curves defined for the Corniglio case history by means of straightforward numerical computations with the observed building damage.

## 2 VULNERABILITY ASSESSMENT METHOD

The method proposed in [5] is applicable for the vulnerability assessment of a low-rise RC building located next to the crest of potentially unstable slopes. Usually, the affected structures are subjected to ground induced differential displacement which may cause structural distress and damage. The proposed method, basically based on numerical simulation and statistical analysis, is applied to earthquake induced landslides but in principle it can be easily modified to account for other triggering mechanisms (e.g. intense precipitation, erosion etc.). In terms of numerical computations, a two-step analysis is performed. In the first step, the deformation demand, i.e. total and/or differential displacements considering the actual weight and stiffness of the building and its foundation system due to the landslide displacement (hazard) is assessed, by means of non-linear finite difference dynamic analyses. In the second step, the building response to the statically imposed landslide differential displacement is estimated

by using a Finite Element code. Four damage limit states, which describe the exceedance of slight, moderate, extensive and complete structural damage of the building (respectively LS1, LS2, LS3, LS4), were defined in terms of threshold values of structural resistance by engineering judgment and pertinent literature investigation [8,9,10]. Different limit strains are adopted for “low” and “high” code designed structures. Then, vulnerability was assessed as log-normally distributed fragility functions, which describe the probability ( $P_i$ ) of exceeding a limit state ( $LS_i$ ) of the building, on a given slope, with respect to a given landslide intensity measure: the fragility parameters for each limit state are estimated as a function of peak ground acceleration (PGA) recorded on rock outcrop or the permanent ground displacement (PGD) at the slope area by correlating the structural response, in terms of strains, with the corresponding values assigned for each damage limit state.

In order to define a set (abacus) of fragility curves applicable to different RC building types, soil conditions and slope configurations, an extensive parametric investigation was performed on the basis of the proposed two-step numerical approach. A set of fragility curves to be used for several engineering applications is suggested, based on the parameters that have been proved to most significantly contribute to the structural vulnerability [6].

### 3 APPLICATION TO CORNIGLIO CASE HISTORY

#### 3.1 Landslide movement and building damage data in Corniglio village

The Corniglio Village is located in the northern part of the Appennines, at an altitude of about 700 m a.s.l., between the towns of Parma and La Spezia (as shown in the map of Fig. 1). The morphology of the area of interest shows the characteristics features of an Appennine mountain site, with steep slopes alternating with narrow and deep valleys.

The time period of interest in the present study spans from September 1994 to December 1999, and was characterised by a nearly continuous landslide activity. During this period, the major re-activations of the landslide (the so-called “Lama”, i.e. “blade”, and nearby portions, see Fig. 1) were recognised to depend on two combined triggering factors:

- Intense rainfalls, particularly before the activation of Dec. 1995 and during November 1996;
- Weak and moderate earthquake ground motion, particularly on occasion of the Correggio Earthquake of October 1996, of magnitude  $M=5.4$ , at an epicentral distance of some 70 Km.

Through the entire period considered, the observed displacements reached tens of m on the main slide body, the so-called “Lama”, while in the adjacent Corniglio Village (the main subject of the present research) the surface ground movements measured by the inclinometers reached typically 20 to 25 cm resulting to moderate/significant damage to the buildings located in the old centre of the village. In particular, the Corniglio Village was affected by two different slide movements: a deep rock block slide (along cross section A-A, see Fig.1) and a surface rotational landslide (cross section B-B). The geological profile of B-B cross section, on which this study is focused, is presented in Figure 2 [11]. Several re-activations of the landslides have affected Corniglio village damaging buildings, roads and other infrastructures. The landslide movements have been attributed mainly to a decrease of geomechanical parameters, caused by the weathering process due to intense precipitations and weak and moderate seismic activity.

A substantial set of instrumental observations has been gathered mainly from the Emilia Romagna Regional Administration in charge of the monitoring and surveillance activities, including the execution of inclinometer readings (monitoring ground movements in free field), geodetic levelling data on several buildings located within the village area and crack aperture

measurements in which damage revealed to be important. The inclinometers location, the position of the geodetic targets (and their ID's) and, for each building monitored, a letter from A to Z between brackets which indicates the crack meters installed, are depicted in Figure 3. The most damaged buildings are denoted by red filled polygons. The processing of the data set was conducted by Callerio et al. [7], focusing on establishing a correlation among ground displacement, building movements and damage induced during sliding so as to provide the basis for a probabilistically sound vulnerability assessment framework. The damage levels observed in Corniglio were defined in terms of ease of repair, based on the scale proposed by Standing et al. [12], identifying 3 damage levels: negligible to slight, slight to moderate and moderate to severe. The ease of repair was then related to the measure of cracks opening.

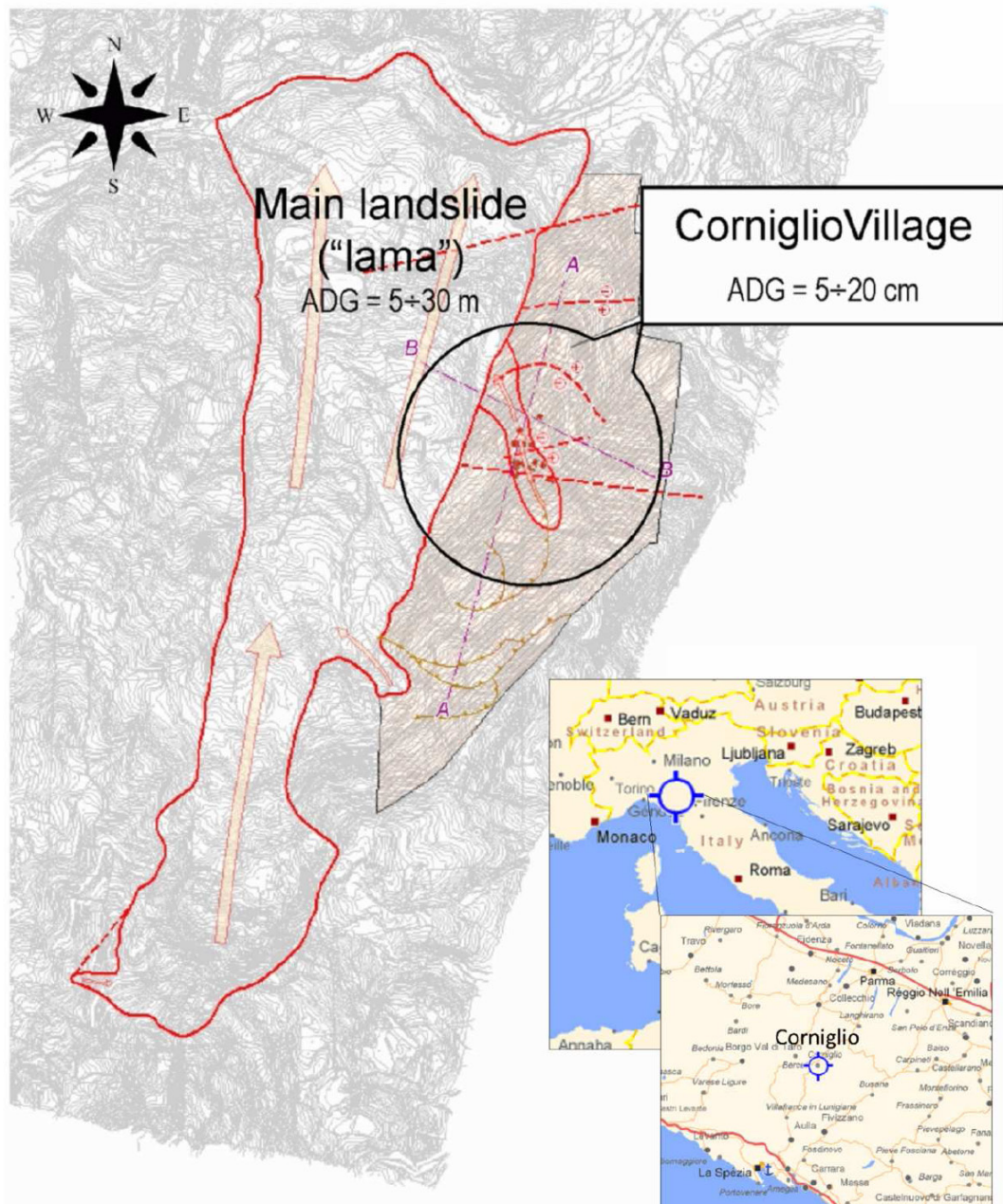
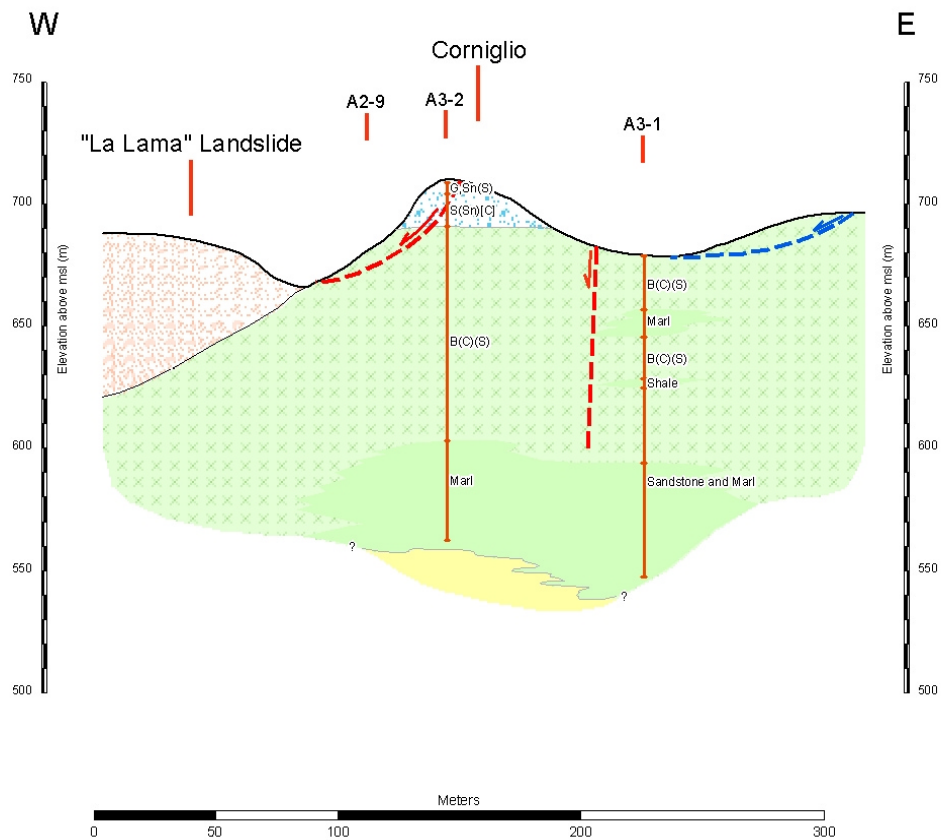


Figure 1: General plan of the area of Corniglio affected by the landslide phenomena during the years 1995-2000. The indicated displacements (ADG = Absolute Ground Displacement) are obtained by aerial photo interpretation ("Lama" area) and inclinometer readings (Village) [7].



### Geology

- Mt. Caio Flish  
*Alternations of limestones and marl layers*
- "Ponte Bratica Sandstone"  
*Alternations of sandstones and silty clays*
- "Ponte Bratica Sandstone"  
*Alternations of sandstones and silty clays - Breached layers*
- "La Lama" landslide
- "Lago Chaotic Unit"  
*Clay shales with calcareous layers*
- Slope deposits  
*Sandy silty gravel, with sandy clayey silt layers*
- Faults
- Ancient or dormant slides
- Surface of rupture
- Surface of sacking

### Geological Investigations

- G** = Gravel
- Sn** = Sand
- S** = Silt
- C** = Clay
- B** = Breached Marl

Figure 2: Soil profile along B-B cross section (see Fig. 1) [11].



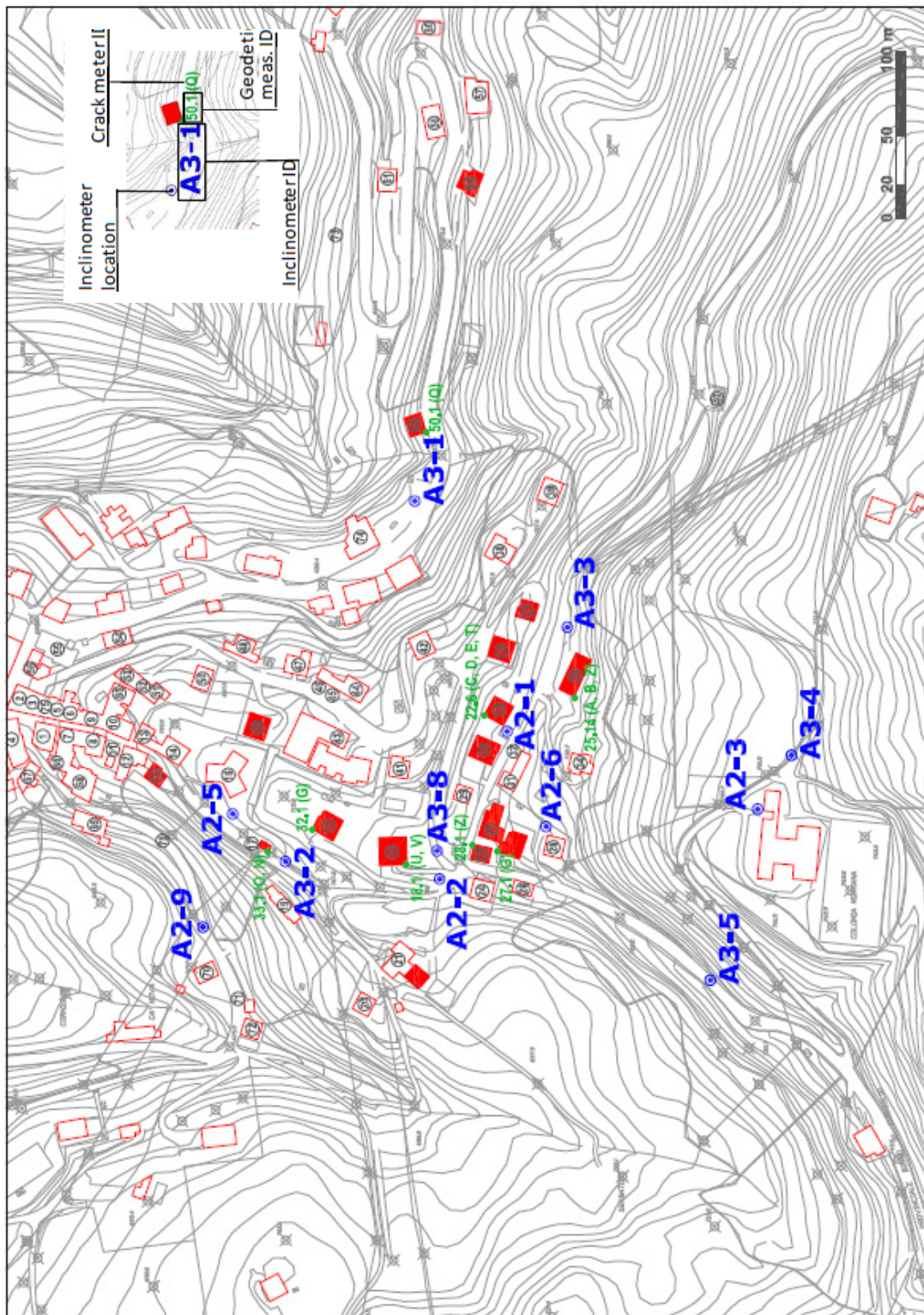


Figure 3: Location of inclinometers, geodetic and crack measurements on buildings. Buildings are denoted by red polygons, whereas the ones that suffered major damages due to the landslide movement are filled in red [7].

### 3.2 Comparison of the observed building damage with the damage predicted by the proposed and simulated fragility curves

The present study is focused on the fragility analysis of an electrical building (n. 17) due to its proximity to the inclinometer A3-2 (see Fig. 3), which is installed near the slope crown of the geotechnical profile B-B of the Corniglio case history (see Fig. 2). Building n. 17 can be considered a rather simple two-storey RC frame structure with masonry infill walls, which suffered considerable structural damage due to the continuous landslide activity. Figure 4a illustrates representative observed physical damage of the building, while Figure 4b shows the location on a map of the building and the nearby inclinometer A3-2. Despite the proximity of another building (n.18) to the inclinometer A3-2, an upper class mansion with well maintained masonry bearing wall structure with an heavy roof, this was not considered as appropriate for the herein fragility analysis, concentrated on RC buildings. Figure 5 displays the ground displacement measured by inclinometer A3-2, the building movement measured by geodetic leveling and the opening of each crack monitored on the structure [7]. The plot is over imposed on the damage scale in terms of cracks opening, to assess the expected damage state of the building. A rather linear relationship between the building movement and crack opening is detected.

As expected, the given data do not exactly fit those at the base of the calculation of fragility curves derived through numerical parametric analysis [6]. In particular, the studied slope configurations do not match very precisely to the given finite slope geometry and soil geotechnical properties of Corniglio case history (see Fig. 2, geotechnical profile B-B: average slope inclination  $\approx 37^\circ$ , average height  $\approx 43$  m). Moreover, first-time failures were analyzed in Fotopoulou and Pitilakis [6] in the presence of a sliding surface allowed to be freely developed, as opposed to the Corniglio case study where the landslide movement is rather complex. Considering all the above, two different approaches of increased complexity for the fragility analysis of building n. 17 in Corniglio village are presented.

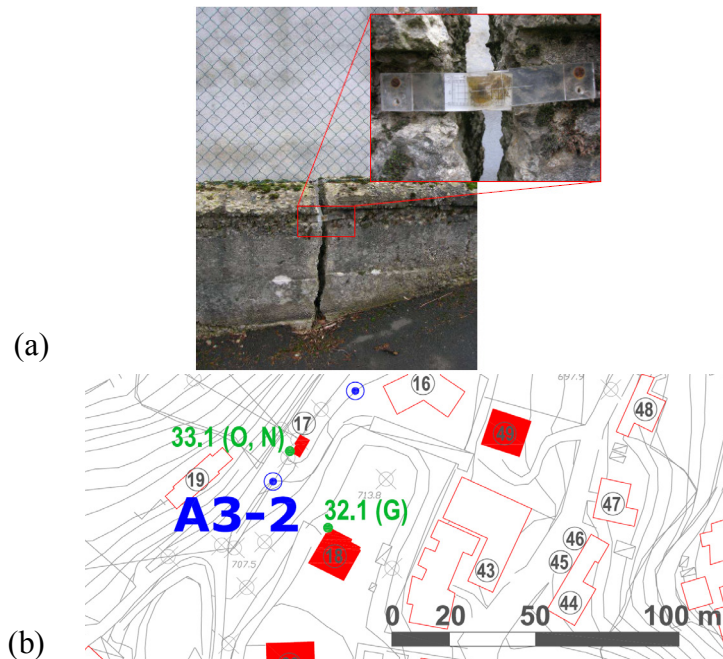


Figure 4: (a) Observed physical damage of building n. 17. (b) Closer view of the building under study and the nearby inclinometer A3-2 within the Corniglio area. The geodetic and crack monitored points on the building are also shown (in green) [7].



Figure 5: Correlation between absolute ground displacement (from nearby Inclinator A3-2), building n. 17 displacement (from geodetic levelling) and crack opening (compared to the defined damage levels) as a function of time [7].

### 3.3 Reliability assessment of the proposed fragility curves

As a first step analysis, two sets of the already developed fragility curves [6] were selected, among those more representative for the Corniglio case history, to be compared with the observed building damage, for the measured level of building displacement (see Fig. 5). These curves have been developed for:

- slope height: 40 m,
- slope inclinations: 30° and 45° respectively
- sandy slope materials
- low code RC frame buildings with flexible foundations

A graph of the aforementioned developed curves is shown in Figure 6 for slope inclinations 30° and 45° respectively. It can be noted that the fragility curves are here presented as a function of the maximum permanent displacement at the foundation level to allow for a direct application to the data available, considering the site-specific nature of the problem under study. The derived lognormal median and dispersions of the fragility functions are given in Table 1. It is worth noting that the adoption of the steel and concrete strain as a damage index in this research [5] implies a structural damage (e.g. in terms of cracks) and a subsequent ductile failure of the building members. This is certainly the case for building n. 17 where extensive cracking was recorded (see Fig. 5).

The damages predicted by the curves are compared with that observed in building n. 17 for the measured level of displacement, i.e. 0.121 m. As shown in Figure 5, for this level of displacement, the building would be in “*moderate to severe*” damage level according to the damage states proposed in Callerio et al. [7].



The proposed curves predict “*slight to moderate*” to “*moderate to extensive*” damages that are in relatively good correlation with the corresponding assigned damage levels based on the field measurements and observations. As it can be easily seen in Figure 6, the expected damages when using the curves derived for 45° slope inclinations are more in line with the observed structural performance. In particular, the estimated probabilities of exceeding slight (LS<sub>1</sub>) and moderate (LS<sub>2</sub>) damage states are 1.0 and 0.4 respectively for the curves referring to the 45° inclined slope, whereas the corresponding probabilities are 0.84 and 0.08 respectively for the curves referring to the 30° inclined slope.

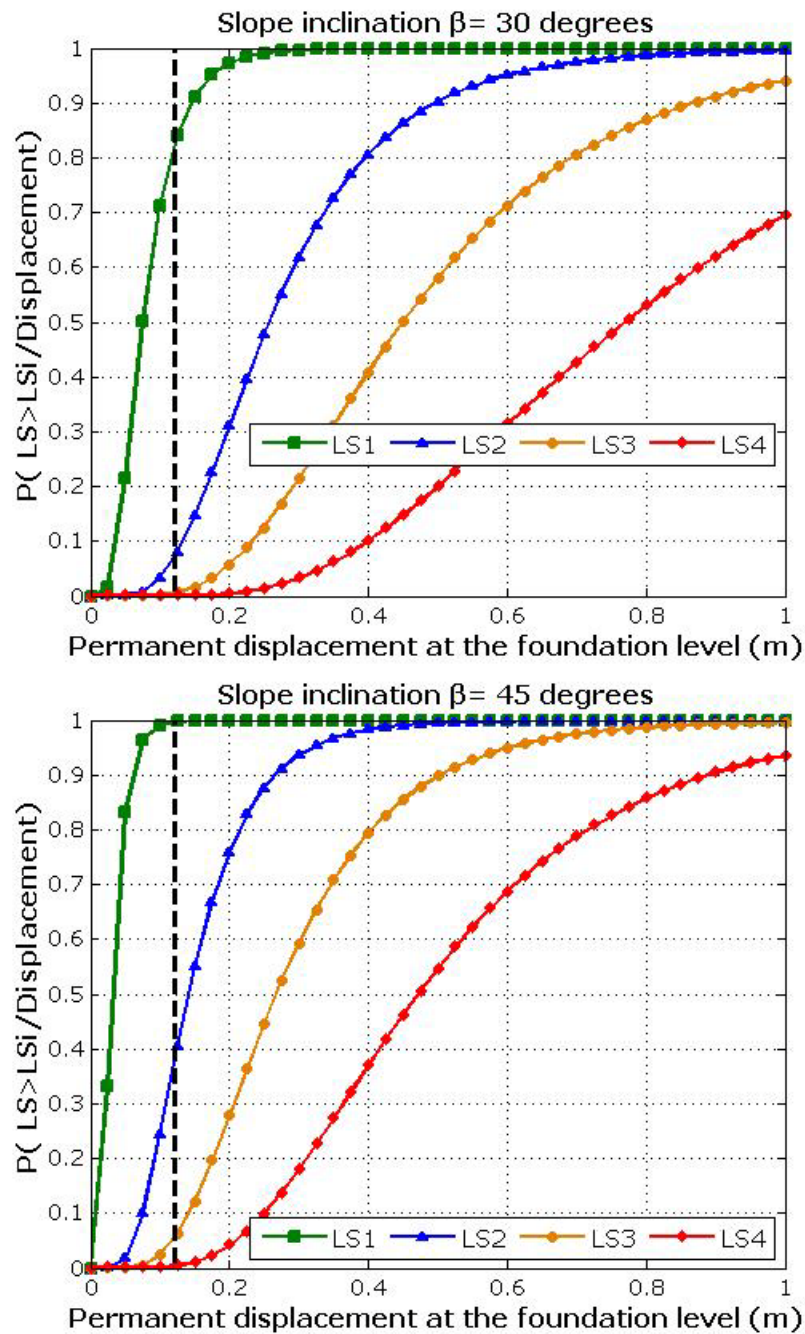


Figure 6: Representative fragility functions derived from the parametric analyses

Limit strain	Displacement at the foundation level (m)			
	Slope inclination angle $\beta=30^\circ$		Slope inclination angle $\beta=45^\circ$	
	Median	Dispersion $\beta$	Median	Dispersion $\beta$
Limit State 1	0.075		0.031	
Limit State 2	0.257	0.51	0.141	0.49
Limit State 3	0.450		0.267	
Limit State 4	0.770		0.472	

Table 1: Parameters of the lognormal distribution for representative fragility functions

### 3.4 Fragility curves for the Corniglio case history- Comparison with recorded damage data

Considering the relatively crude approximation that it may be achieved with the comparisons presented above a more sophisticated analysis resulting to the development of more appropriate fragility curves for the Corniglio case history based on the data provided (e.g. geotechnical profile B-B, inclinometer A3-2 records associated with building n.17 geodetic and crack measurements) was carried out. Fragility curves were derived from the study of the response of the slope to earthquake shaking, which in our case is the permanent cumulative ground displacement at the foundation level. This is a commonly used landslide intensity measure, which may sufficiently describe the destructive effect of a relatively slow-moving slide to a structure located within the landslide zone [13]. The final deformation demand for the building is given in terms of the corresponding differential displacement, which better describe the induced damage to the building. The ultimate goal of the analysis was to define more reliable correlations between the observed and simulated damage of the building for the measured displacement level so as to increase the reliability of the developed method [5].

The two-step numerical analysis as described in Fotopoulou and Pitilakis [5] was performed. Numerical codes FLAC2D 7.0 [14] and SEISMOSTRUCT [15] were used for the slope-foundation dynamic and structure's quasi-static analyses respectively.

Taking into account the various uncertainties related to the lack of a detailed geotechnical investigation, the simplified finite slope geometry shown in Figure 7 was adopted to describe the geotechnical profile B-B; the simplified model is characterized by three layers with different material properties (Soil 1, Soil 2, elastic bedrock) and a pre-existing sliding surface (Slide). The water table was assumed to lie at the base of the slope (-43m).

The soil materials overlaying the elastic bedrock were modelled through the adoption of an elasto-plastic constitutive law with a Mohr-Coulomb limit surface, coupled to an hysteretic damping scheme. In particular, FLAC 7.0 hysteretic damping formulation was implemented by selecting the "default" model to account for a nonlinear hysteretic soil behavior. The model fits the damping and shear modulus curves over a reasonable range of strains (e.g. up to 0.2-0.3%) which are expected to occur. In particular, the Seed and Idriss [16] sand-upper range curves were used for the slide material and the upper soil formation (Soil 1), whereas Sun et al. [17] clay-upper range curves were used for Soil 2. A small amount (e.g. 0.2%) of stiffness-proportional Rayleigh damping was also added to compensate for the low damping demonstrated by the program at small strains. In addition, for the elastic bedrock materials a constant 0.5% of Rayleigh-type damping was assigned. The geotechnical parameters of the soil formations for the assumed 2D cross-section are summarized in Table 2.

Free field boundary condition was applied along the vertical boundaries of the model, while a quiet (viscous) boundary was applied at the bottom in order to minimize the effect of artificially reflected waves [14]. The FLAC 2D grid and boundary conditions are schematically illustrated in Figure 8.

A single span, two storey, reinforced concrete building is assumed to be located at 10 m from the crest to approximately model building n. 17. No relative slip or separation between the structure and the underlying soil materials was allowed. The assumed bay length and storey height were 5 m and 3m respectively.

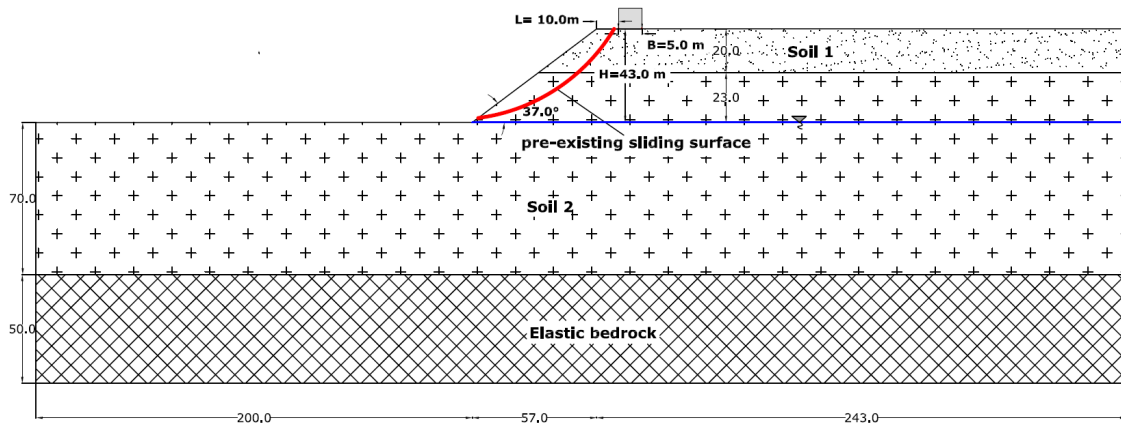


Figure 7: Slope configuration adopted for the geotechnical profile B-B

	Soil 1	Slide	Soil 2	Elastic bedrock
Soil thickness (m)	20	1.0-2.0	93	40
Density $\rho$ (kg/m <sup>3</sup> )	1800	1700	2000	2300
Young's modulus E (KPa)	2.93E+05	4.42E+04	1.30E+06	4.32E+06
Poisson's ratio $\nu$	0.3	0.3	0.3	0.3
Bulk modulus K (KPa)	2.44E+05	3.68E+04	1.08E+06	3.60E+06
Shear modulus G (KPa)	1.13E+05	1.70E+04	5.00E+05	1.66E+06
Cohesion (KPa)	10	8	50	-
Friction angle (degrees)	35	35	30	-
Shear wave velocity $V_s$ (m/sec)	250	100	500	850
Max. allowed zone size (m)	2.5	1	5	8.5
Max. Allowed frequency	10	10	10	10

Table 2: Assumed soil properties for the geotechnical profile B-B

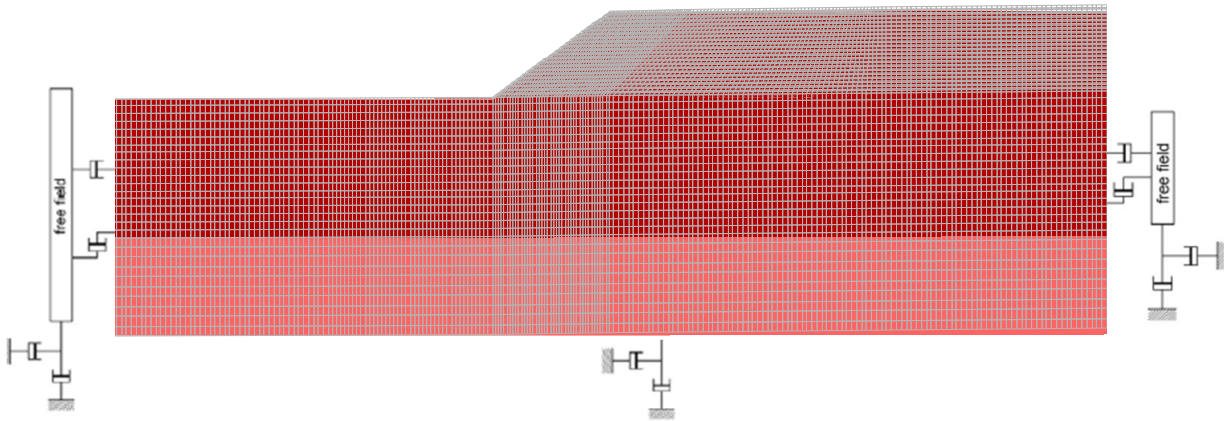


Figure 8: Simplified 2D FLAC dynamic model adopted for the geotechnical profile B-B

Earthquake Name	Country	Date	R (km)	M <sub>w</sub>	Station Name	V <sub>s,30</sub> (m/s)	Database Code
Kalamata (Aftershock)	Greece	10/6/1987	17	5.36	Kyparrisia-Agriculture Bank	778	ESMD_126_H1
Ano Liosia	Greece	7/9/1999	17	6.04	Athens 4 (Kipseli District)	934	ESMD_335_H1
Kozani (After-shock)	Greece	17/5/1995	16	5.3	Chromio-Community Building	623	ISESD_1210_H1
Friuli	Italy	6/5/1976	21.7	6.4	Tolmezzo-Diga Ambiesta	1030	ITACA_16_H1
Friuli (After-shock)	Italy	15/9/1976	8.5	5.9	Tarcento	901	ITACA_116_H1
Umbria Marche (Aftershock)	Italy	14/10/1997	20	5.6	Norcia	681	ITACA_491_H2
App. Lucano	Italy	9/9/1998	6.6	5.6	Lauria Galdo	603	ITACA_613_H2
L Aquila Mainshock	Italy	6/4/2009	4.4	6.3	L Aquila - V. Aterno - Colle Grilli	685	ITACA_857_H2
San Fernando	USA	9/2/1971	20.04	6.61	Lake Hughes #12	602	NGA_71_H2
Coyote Lake	USA	6/8/1979	4.37	5.74	Gilroy Array #6	663	NGA_150_H2
Morgan Hill	USA	24/4/1984	36.34	6.19	Gilroy Array #6	663	NGA_459_H2
Loma Prieta	USA	18/10/1989	35.47	6.93	Gilroy Array #6	663	NGA_769_H1

Table 3: Ground motion records used in the numerical simulations derived from the SHARE database [17]



Prior to the dynamic simulations, a static analysis was carried out in order to establish the initial effective stress field throughout the model; a stationary ground flow analysis was also performed to assess the pore pressure distribution.

The seismic input applied along the base of the model consisted of a set of 13 real acceleration time histories from SHARE database ([18]; <http://www.share-eu.org/>), recorded during Italian, Greek and USA earthquakes on stiff soils, characterized by an average shear wave velocity in the upper 30 m,  $V_{s,30}$ , greater than 600 m/sec (Table 3). The 5%-damped acceleration response spectra of the selected records as well as the corresponding average and median spectra are shown in Figure 9.

To define the appropriate input motion to be applied at the base of the FLAC model, the selected time histories were first corrected with respect to baseline and filtered (band pass within 0.25 and 10 Hz) allowing for an accurate representation of wave transmission through the model by choosing a maximum propagated frequency of 10Hz by spacing the grid accordingly. Moreover, due to the compliant base used in the model, the appropriate input excitation corresponds to the upward propagating shear wave that is taken as one-half the target outcrop motion [19]. The selected input time histories were scaled to three levels of peak ground acceleration, namely  $PGA=0.1, 0.15, 0.2g$  in order to assess the building response for different ground differential displacement magnitudes, to study different damage states and construct the corresponding fragility curves. It is worth noting that that, due to the presence of a pre-existing sliding surface, the required amplitudes of the input excitations able to cause extensive slope and foundation deformations are generally lower than the corresponding amplitude considered in the case of first-time failures, as performed in Fotopoulou and Pitilakis [5].

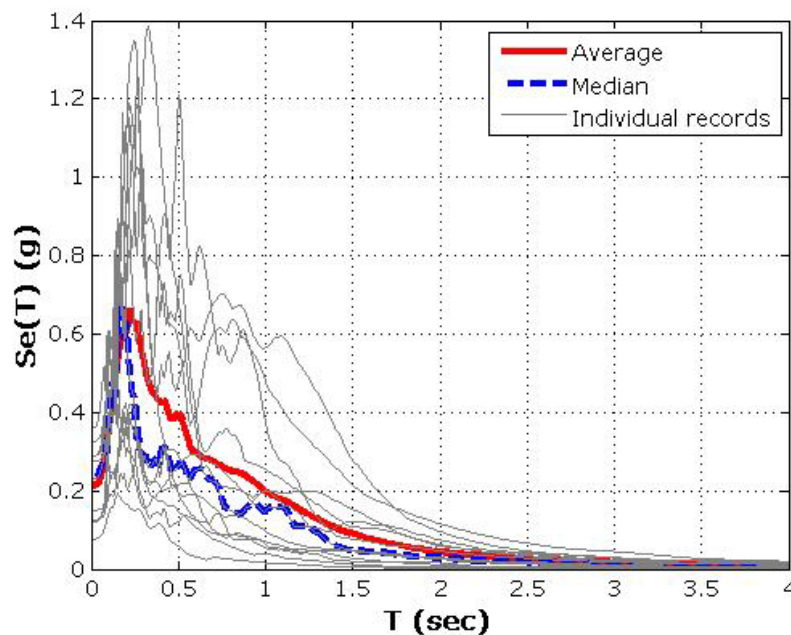


Figure 9: Linear 5%-damped acceleration response spectra of the records selected for numerical analyses. The average and median spectra are also shown.

Figures 10(a) and 10(b) depict the derived horizontal and vertical differential displacements time histories respectively at the closest edge of the assumed building from the slope's crest (i.e. 10 m), for input accelerograms scaled at 0.15 g. It is observed that the specific characteristics (frequency content and duration) of the seismic ground motions can significantly

affect the history and the amplitude of the computed differential displacement demand at the foundation level.

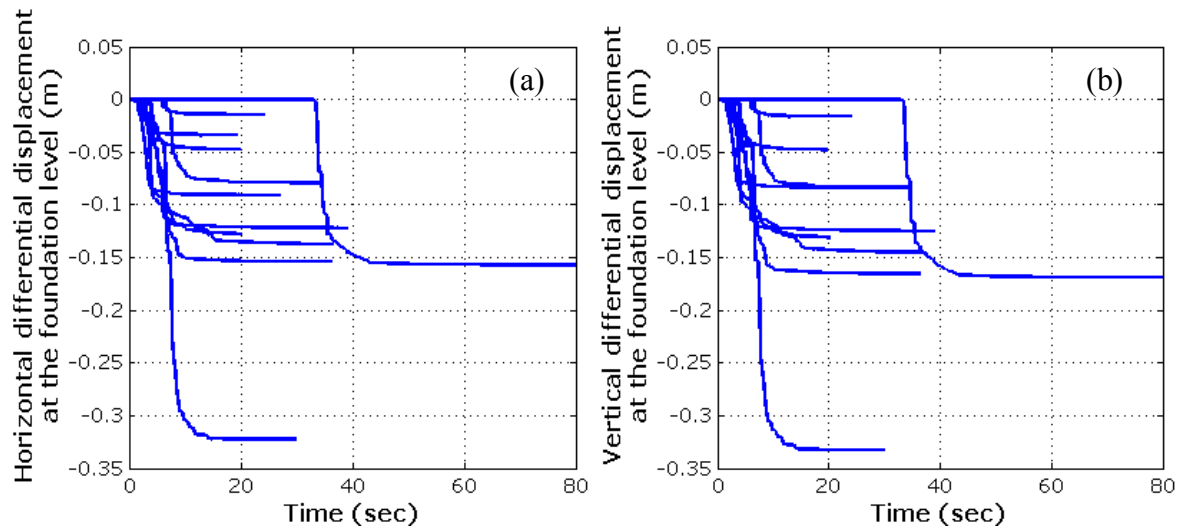


Figure 10: Differential horizontal (a) and vertical (b) ground displacements at the building's foundation level for input accelerograms scaled at 0.15 g.

Then, a non-linear quasi-static analysis was performed on the 1 bay-2 storey RC frame building model of Fig. 11 by means of the finite element code SEISMOSTRUCT [15]. More specifically, the derived differential displacement time histories extracted from FLAC dynamic analysis (see Fig. 10) were directly applied quasi-statically at one of the RC frame supports. The beneficial contribution of masonry infill walls to the building capacity was not considered in this study.

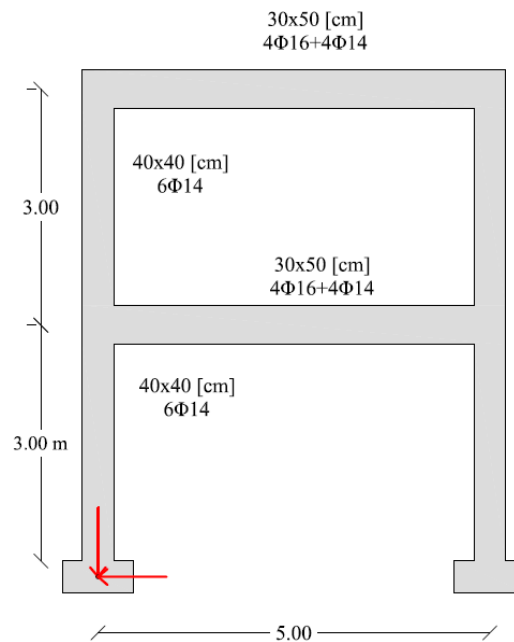


Figure 11: Schematic view of the studied building in Corniglio village and displacement loading pattern considered for the non-linear quasi-static analysis

Non-linear fiber-based material properties were assumed for the structural members of the RC frame building under investigation. More specifically, a uni-axial, nonlinear model considering a constant confining pressure throughout the entire stress-strain range was used for the concrete material [20] (parameters:  $f_c=20\text{MPa}$ ,  $f_t=2.1\text{MPa}$ , strain at peak stress  $0.002\text{mm/mm}$ , confinement factor  $=1$  for unconfined and  $1.2$  for confined concrete, specific weight  $=24\text{KN/m}^3$ ) and a uni-axial bilinear stress-strain model with kinematic strain hardening was used for the reinforcement (parameters:  $f_y=400\text{MPa}$ ,  $E=200\text{GPa}$ , strain hardening parameter  $\mu=0.005$ , specific weight  $=78\text{KN/m}^3$ ).

Then, structural response data were statistically put in relation with the corresponding limit damage states and landslide intensity parameter in order to estimate structure's fragility curves. Figure 12 depicts a representative plot of damage evolution expressed in terms of maximum steel strain (damage index) as a function of the expected maximum permanent ground displacement at the foundation level for the low-rise, "low code" designed RC frame building. The figure also shows the limit steel strains needed to exceed yield and post-yield limit states for low-code RC buildings characterized by a low level of confinement, as defined in Fotopoulou and Pitilakis [5].

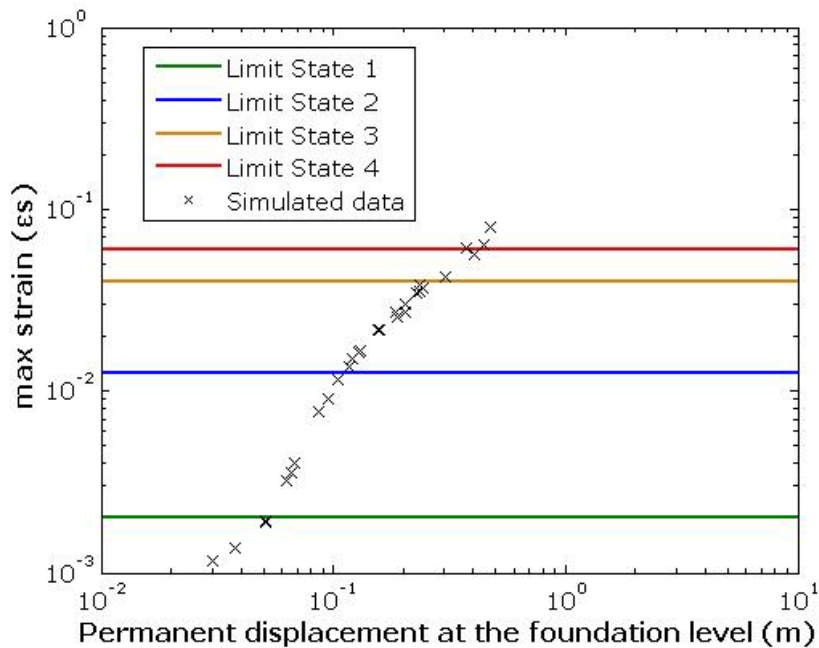


Figure 12: Maximum recorded steel strain as a function of permanent ground displacement at the foundation level for the studied building in Corniglio village

	Permanent displacement at the foundation level (m)	
	Median (m)	Dispersion $\beta$
Limit State 1	0.042	0.41
Limit State 2	0.093	
Limit State 3	0.168	
Limit State 4	0.315	

Table 4: Parameters of fragility functions for the studied building in Corniglio village

Finally, probabilistic fragility curves in terms of permanent displacement at the foundation level for building n. 17 in Corniglio village were derived with the aid of the Maximum likelihood Method (see [6] for details). Table 4 presents the lognormal parameters of the fragility functions, whilst Figure 13 depicts the corresponding plots. The simulated fragility curves predict that the building n. 17 studied herein is more likely to suffer “*moderate to extensive damage*”, for the measured level of displacement, i.e. 0.121 m. In particular, the estimated probabilities of exceeding moderate (LS2) and extensive damage (LS3) are 0.85 and 0.22 respectively. These observations are in fairly good agreement with the observed building damages (see Fig. 5), verifying in this specific case characterized by an extensive amount of observational data, the validity of the derived fragility curves, finally enforcing the robustness of the developed methodological framework [5].

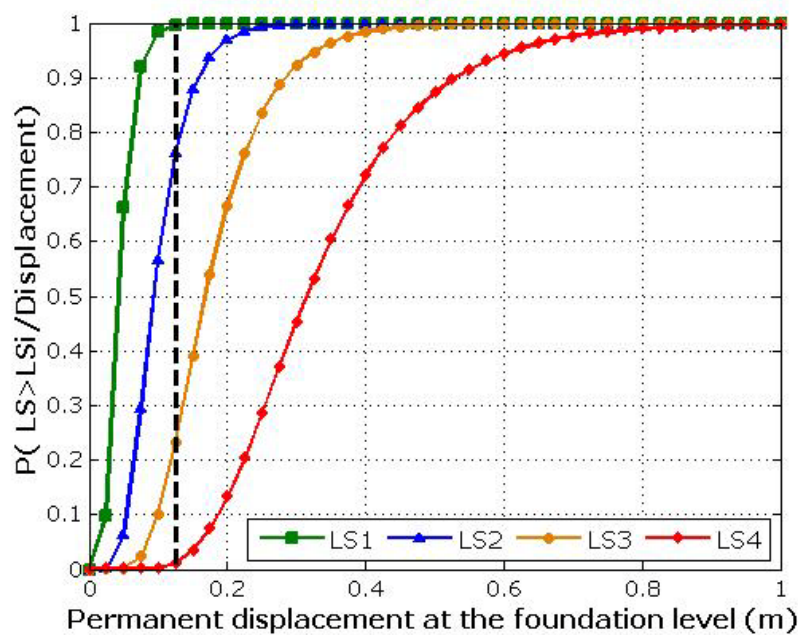


Figure 13: Fragility curves for the studied RC frame building in Corniglio village

#### 4 CONCLUSIONS

The reliability and applicability of the developed methodology for assessing the vulnerability of low-rise RC buildings to earthquake induced landslide displacements has been assessed through its application to a representative RC building in Corniglio village-Italy. The studied building suffered moderate to extensive structural damage due to the landslide movement, well documented during and after the landslide event. The direct comparison of the observed damage with that predicted by the previously developed representative fragility functions proved that the suggested fragility curves could adequately capture the performance of the representative RC building which was affected by the slope co-seismic landslide differential displacement. In addition, to enhance the effective implementation of the proposed methodological framework within a probabilistic risk assessment study, more appropriate fragility curves were constructed for the studied building in Corniglio village based on straightforward numerical computations. The obtained fragility curves were compared to the observed build-



ing damage for the measured level of displacement. Although such a comparison revealed to be quite promising, a further validation of the proposed method on building damage data from past landslide events is certainly warranted to reinforce its reliability and accuracy in predicting damage levels for a certain exposure of the building and intensity of the landslide event.

## REFERENCES

- [1] F.C. Dai, C.F. Lee, Y.Y. Ngai, Landslide risk assessment and management: an overview, *Engineering Geology*, **64**(1), 65-87, 2002.
- [2] J. Remondo, J. Bonachea, A. Cendrero, Quantitative landslide risk assessment and mapping on the basis of recent occurrences, *Geomorphology*, **94**, 496-507, 2008.
- [3] J.L. Zêzere, R.A.C. Garcia, S.C. Oliveira, E. Reis, Probabilistic landslide risk analysis considering direct costs in the area north of Lisbon (Portugal), *Geomorphology*, **94**, 467-495, 2008.
- [4] C.J. Van Westen, T.W.J. Van Asch, R. Soeters, Landslide hazard and risk zonation—why is it still so difficult?, *Bulletin of Engineering Geology and the Environment*, **65**, 167-184, 2006.
- [5] S. Fotopoulou, K. Pitilakis, Vulnerability assessment of reinforced concrete buildings subjected to seismically triggered slow-moving earth slides, *Landslides*, 2012 (DOI: 10.1007/s10346-012-0345-5).
- [6] S. Fotopoulou, K. Pitilakis, Fragility curves for reinforced concrete buildings to seismically triggered slow-moving slides. *Soil Dynamics and Earthquake Engineering*, 2013, <http://dx.doi.org/10.1016/j.soildyn.2013.01.004>
- [7] A. Callerio, E. Faccioli, A. Kaynia, *Deliverable 121: Landslide risk assessment methods and applications (III) – Application to real active landslides – Phase II (68pp)*. LESSLOSS integrated project: Risk Mitigation for Earthquake and Landslides, Sub-Project 4 – Landslide risk scenarios and loss modelling, 2007.
- [8] H. Crowley, R. Pinho, J.J. Bommer, A probabilistic displacement-based vulnerability assessment procedure for earthquake loss estimation, *Bulletin of Earthquake Engineering*, **2**(2), 173-219, 2004.
- [9] J.F. Bird, H. Crowley, R. Pinho, J.J. Bommer, Assessment of building response to liquefaction induced differential ground deformation, *Bul of the New Zealand Society for Earthquake Engineering*, **38**(4), 215-234, 2005.
- [10] C. Negulescu, E. Foerster, Parametric studies and quantitative assessment of the vulnerability of a RC frame building exposed to differential settlements, *Natural Hazards and Earth System Sciences*, **10**, 1781-1792, 2010.
- [11] Lessloss, *The Corniglio landslide (Parma - Italy): Geological data*, Studio Geotecnico Italiano, 28 April, Milan, 2005.
- [12] J.R. Standing, T.I. Addenbrooke, J.B. Burland, The assessment and building response to tunneling, risk of damage and structural monitoring, L.G.W. Verhoef ed., *Proc. of International Congress on Urban Heritage and Building Maintenance: Foundations*, Delft University of Technology, 1999.

- [13] F. Leone, J.P. Aste, E. Leroi, *Vulnerability assessment of elements exposed to mass moving: working towards a better risk perception*. In K. Senneset (Ed.), *Landslides*, Balkema, Rotterdam. pp. 263-269, 1996.
- [14] Itasca Consulting Group, Inc. *FLAC (Fast Lagrangian Analysis of Continua)*, ver. 7.0, Itasca Consulting Group, Inc., Minneapolis, 2011.
- [15] SeismoSoft, SeismoStruct, *A computer program for static and dynamic nonlinear analysis of framed structures*. Available from URL: [www.seismosoft.com](http://www.seismosoft.com).
- [16] H.B. Seed, I.M. Idriss, *Soil moduli and damping factors for dynamic response analyses*, Univ. of California, Berkeley, California, Report No. EERC 70-10, 1970.
- [17] J.I. Sun, R. Golesorkhi, H.B. Seed, *Dynamic moduli and damping ratios for cohesive soils*, Earthquake Engineering Research Center, University of California, Berkeley, Report No. UCB/EERC-88/15, p. 42, 1988.
- [18] E. Yenier, M.A. Sandikkaya, S. Akkar, *Report on the fundamental features of the extended strong motion databank prepared for the SHARE project (v1.0)*, 2010.
- [19] L.H. Mejia, E.M. Dawson, Earthquake deconvolution for FLAC. *Proc. 4th International FLAC Symposium*, Madrid, Spain, 211-219, 2006.
- [20] J.B. Mander, M.J.N. Priestley, R. Park, Theoretical stress-strain model for confined concrete, *Journal of Structural Engineering*, **114**(8), 1804-1826, 1988.